nature immunology

VAMP7 controls T cell activation by regulating the recruitment and phosphorylation of vesicular Lat at TCR-activation sites

Paola Larghi[1,2], David J Williamson[3], Jean-Marie Carpier[1,2], Stéphanie Dogniaux[1,2], Karine Chemin[1,2,6], Armelle Bohineust[1,2], Lydia Danglot[4,5], Katharina Gaus[3], Thierry Galli[4,5,7] & Claire Hivroz[1,2,7]

The mechanisms by which Lat (a key adaptor in the T cell antigen receptor (TCR) signaling pathway) and the TCR come together after TCR triggering are not well understood. We investigate here the role of SNARE proteins, which are part of protein complexes involved in the docking, priming and fusion of vesicles with opposing membranes, in this process. Here we found, by silencing approaches and genetically modified mice, that the vesicular SNARE VAMP7 was required for the recruitment of Lat-containing vesicles to TCR-activation sites. Our results indicated that this did not involve fusion of Lat-containing vesicles with the plasma membrane. VAMP7, which localized together with Lat on the subsynaptic vesicles, controlled the phosphorylation of Lat, formation of the TCR-Lat-signaling complex and, ultimately, activation of T cells. Our findings suggest that the transport and docking of Lat-containing vesicles with target membranes containing TCRs regulates TCR-induced signaling.

The activation of T cells requires direct contact between T lymphocytes and antigen-presenting cells (APCs) at the immunological synapse, where the T cell antigen receptor (TCR) recognizes complexes of peptide and major histocompatibility complex (MHC). The binding of TCRs to peptide-MHC complexes induces clustering of the TCRs and recruitment and activation of the kinases Lck and Zap70 (ζ-chain–associated protein kinase) to the TCR-activation sites[1]. Once recruited, those kinases phosphorylate many signaling proteins, including the signaling adaptor Lat[2,3].

Lat is a transmembrane protein that, after phosphorylation, serves as an adaptor for the formation of various signaling complexes involved in remodeling of the T cell cytoskeleton[4,5], T cell development[6] and T cell activation[7,8]. Hence, the assembly of Lat signaling complexes, also called the 'Lat signalosome'[9], is critical in T cell activation. TCRs and Lat are preclustered in separate domains of the plasma membrane in quiescent cells, which concatenate after antigen recognition[10]. Lat is also present in subsynaptic vesicles that move in a restricted manner and are polarized and translocated to the cell surface after triggering of the TCR[11,12]. Recruitment of this subsynaptic pool of Lat, rather than of the preexisting Lat domains in the plasma membrane, is sufficient for Lat phosphorylation[11,12]. Such results raise the issue of the nature of the molecular machinery involved in the recruitment of the Lat-containing subsynaptic vesicles to the TCR-activation sites. We reasoned that the molecular machinery involved in the recruitment of subsynaptic vesicles to the neurological synapse might also be involved in the recruitment of vesicular Lat to the immunological synapse. SNARE (soluble *N*-ethylmaleimide-sensitive protein-attachment protein receptor) molecules are the core constituents of the machinery that facilitates the fusion of synaptic vesicles with the presynaptic plasma membrane, which results in the release of neurotransmitters[13]. More generally, SNARE molecules are involved in the docking, priming and fusion of opposing membranes[14]. Members of the target family of SNARE proteins (t-SNARE) mark specific organelles, whereas members of the vesicular family of proteins (v-SNARE) localize on donor vesicles. The formation of complexes between t-SNARE proteins and cognate v-SNARE proteins permits close apposition, which can lead to fusion, of the two membranes. Some of these SNARE proteins are inactivated by neurotoxins such as tetanus toxin, whereas others are insensitive to such toxins[15].

We investigated here the role of v-SNARE proteins in recruitment of the vesicular pool of Lat to TCR-activation sites and in the phosphorylation of the vesicular pool of Lat. We found that the recruitment of Lat-containing subsynaptic vesicles to TCR-activation sites depended on the v-SNARE VAMP7 but did not depend on neurotoxin-sensitive SNARE proteins. We also found evidence that Lat-containing subsynaptic vesicles did not fuse with the plasma membrane. VAMP7 localized together with the vesicular pool of Lat and was recruited

[1]Institut Curie, Centre de Recherche, Pavillon Pasteur, Paris, France. [2]Institut National de la Santé et de la Recherche Médicale, Unité 932, Immunité et Cancer, Paris, France. [3]Centre for Vascular Research and Australian Centre for Nanomedicine, University of New South Wales, Sydney, Australia. [4]Institut Jacques Monod, Unité Mixte de Recherche 7592, Centre National de la Recherche Scientifique, Université Paris Diderot, Sorbonne Paris Cité, Paris, France. [5]Institut National de la Santé et de la Recherche Médicale Equipe de Recherche Labelisée U950, Membrane Traffic in Neuronal and Epithelial Morphogenesis, Paris, France. [6]Present address: Department of Medicine, Rheumatology Unit, Center for Molecular Medicine, Karolinska Institutet, Stockholm, Sweden. [7]These authors contributed equally to this work. Correspondence should be addressed to C.H. (claire.hivroz@curie.fr).

Received 15 February; accepted 9 April; published online 12 May 2013; doi:10.1038/ni.2609

together with Lat to the immunological synapse. In the absence of VAMP7, defective recruitment of vesicular Lat to TCR-activation sites was accompanied by a defect in Lat phosphorylation and in antigenic stimulation of T cells. Finally, analysis of TCR-induced signaling showed that VAMP7 controlled the formation of Lat signalosomes. Together the results of our study demonstrate the role of VAMP7 in T cell activation. They also suggest that TCR signal transduction does not rely solely on the reorganization of the molecules in the plasma membrane but also relies on the transport and docking of preexisting vesicular pools of signaling proteins.

RESULTS

VAMP7 controls the recruitment of Lat to TCR-activation sites

Triggering of the TCR induces the recruitment of Lat-containing subsynaptic vesicles to the immunological synapse, which suggests that intracellular pools of Lat may be phosphorylated and thus contribute to T cell activation[5,11,12]. We investigated whether SNARE molecules (which commonly facilitate the docking, priming and fusion of opposing membranes) and in particular VAMP7 were involved in the trafficking of vesicular Lat toward TCR-activation sites. Silencing of the expression of VAMP7 by infection of Jurkat human T lymphocytes (**Fig. 1a**) or primary human CD4$^+$ T cells (**Supplementary Fig. 1a**) with lentivirus encoding either of two different short hairpin RNAs (shRNAs) targeting VAMP7 (Sh1 or Sh5) resulted in lower VAMP7 expression in both cell types. To investigate whether VAMP7 was required for the recruitment of Lat to TCR-activation sites, we incubated T cells for 10 min on coverslips coated with monoclonal antibody (mAb) to CD3 and mAb to CD28, then fixed the cells and imaged them by total internal reflection fluorescence (TIRF) microscopy to detect endogenous Lat. We observed higher concentrations of Lat at the cell surface on activated T cells expressing control shRNA than on those expressing VAMP7-specific shRNA for both Jurkat cells (**Fig. 1b** and **Supplementary Videos 1–3**) and primary T cells (**Supplementary Fig. 1b**). Those results were not due to lower expression of total Lat (**Fig. 1c** and **Supplementary Fig. 1c**). Consistent with published reports[11,12], activation of the TCR by adherent antibodies on poly-L-lysine-coated surfaces induced more recruitment of Lat than did poly-L-lysine alone, in Jurkat cells and primary T cells (**Fig. 1b** and **Supplementary Fig. 1b**). Next, we incubated primary CD4$^+$ T cells from VAMP7-deficient mice[16] or from their wild-type littermates (control mice) for 10 min on coverslips coated with activating antibodies and imaged Lat microclusters by TIRF microscopy. Similar to the results obtained with Jurkat cells in which VAMP7 was silenced, there was significantly less recruitment of Lat to the site of TCR triggering in CD4$^+$ T cells from VAMP7-deficient mice than in those from their wild-type littermates (**Fig. 1d**). This was not due to defective expression of TCR, the invariant signaling protein CD3 or the costimulatory molecule CD28, because both Jurkat cells and human primary T cells in which VAMP7 was silenced and CD4$^+$ T cells from VAMP7-deficient mice had normal expression of these proteins (**Supplementary Fig. 2**).

We next analyzed the potential role of other SNARE molecules in the recruitment of Lat by analyzing the effect of tetanus neurotoxin. This selective protease cleaves a subgroup of v-SNARE proteins (VAMP1, VAMP2 and VAMP3) but not VAMP7 and in doing so inhibits the exocytosis of synaptic vesicles[15].

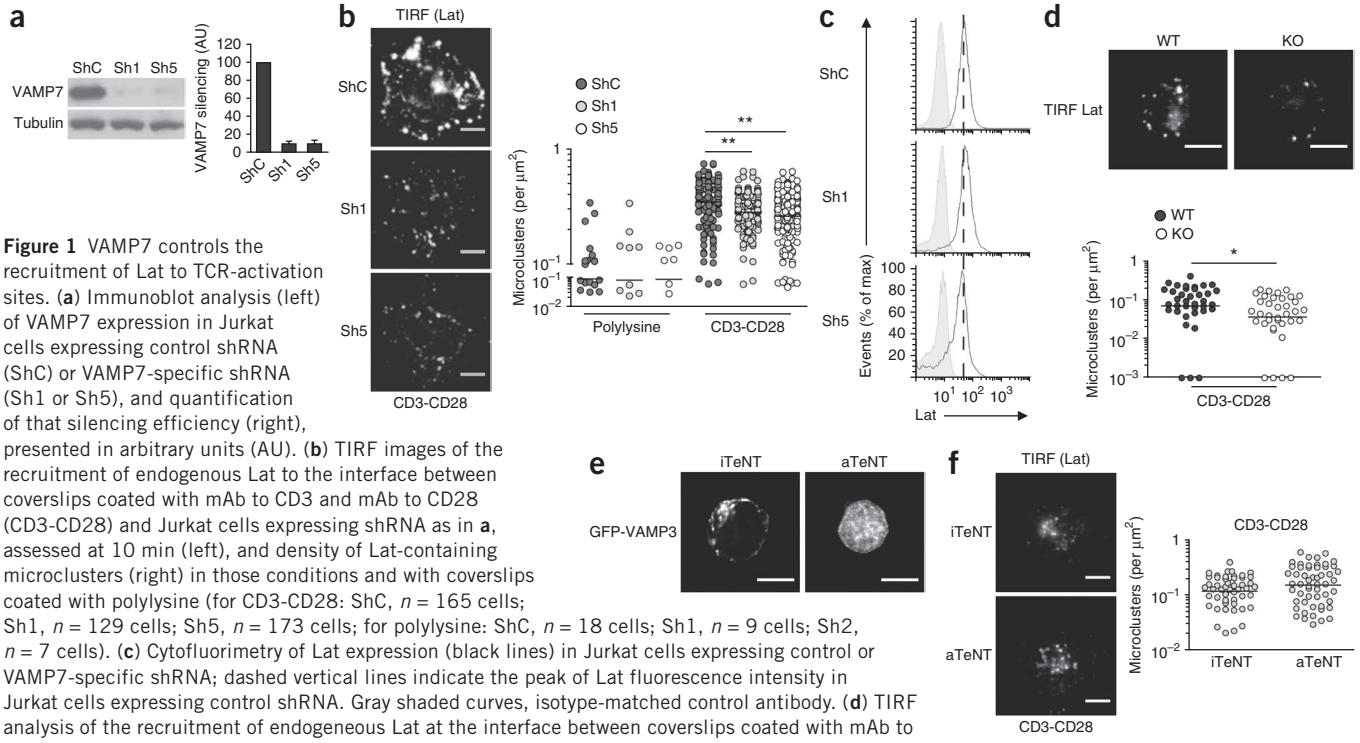

Figure 1 VAMP7 controls the recruitment of Lat to TCR-activation sites. (**a**) Immunoblot analysis (left) of VAMP7 expression in Jurkat cells expressing control shRNA (ShC) or VAMP7-specific shRNA (Sh1 or Sh5), and quantification of that silencing efficiency (right), presented in arbitrary units (AU). (**b**) TIRF images of the recruitment of endogenous Lat to the interface between coverslips coated with mAb to CD3 and mAb to CD28 (CD3-CD28) and Jurkat cells expressing shRNA as in **a**, assessed at 10 min (left), and density of Lat-containing microclusters (right) in those conditions and with coverslips coated with polylysine (for CD3-CD28: ShC, $n = 165$ cells; Sh1, $n = 129$ cells; Sh5, $n = 173$ cells; for polylysine: ShC, $n = 18$ cells; Sh1, $n = 9$ cells; Sh2, $n = 7$ cells). (**c**) Cytofluorimetry of Lat expression (black lines) in Jurkat cells expressing control or VAMP7-specific shRNA; dashed vertical lines indicate the peak of Lat fluorescence intensity in Jurkat cells expressing control shRNA. Gray shaded curves, isotype-matched control antibody. (**d**) TIRF analysis of the recruitment of endogeneous Lat at the interface between coverslips coated with mAb to CD3 and mAb to CD28 and CD4$^+$ T cells from VAMP7-deficient (KO) mice or from their VAMP7-sufficient (WT) littermates, assessed at 10 min (top), and density of Lat-containing microclusters (below: KO, $n = 36$ cells; WT, $n = 37$ cells). (**e**) Deconvoluted images of GFP-VAMP3 in Jurkat T cells expressing GFP-VAMP3 together with inactive mutant tetanus toxin (iTeNT) or proteolytic active tetanus toxin (aTeNT). (**f**) TIRF images of the recruitment of Lat-mCherry to the interface between coverslips coated with mAb to CD3 and mAb to CD28 and Jurkat cells cotransfected with plasmid encoding inactive mutant or proteolytic active tetanus toxin together with plasmid encoding Lat-mCherry (left), and density of microclusters containing Lat-mCherry in those conditions (right: iTeNT, $n = 54$ cells; aTeNT, $n = 55$ cells). Each symbol (**b**,**d**,**f**) represents an individual cell; horizontal lines indicate the geometric mean. Scale bars (**b**,**d**–**f**), 5 μm. $*P \leq 0.01$ and $**P \leq 0.0001$ (Student's *t*-test). Data represent three independent experiments (**a**; mean and s.e.m.), two experiments (**b**,**d**,**e**) or three experiments (**f**) or are from one experiment representative of six (**c**).

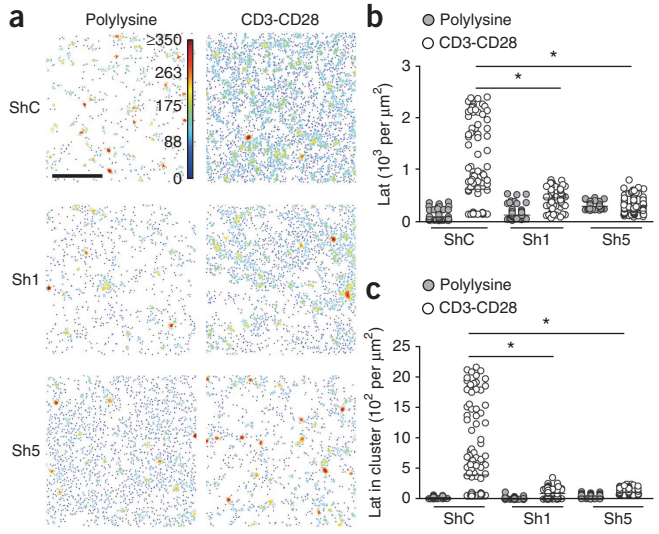

Figure 2 Recruitment and clustering of Lat in cells depleted of VAMP7. (**a**) TIRF-PALM imaging of single molecules of Lat in Jurkat T cells expressing PS-CFP2-tagged Lat and transduced with control or VAMP7-specific shRNA, assessed as resting cells (Polylysine) or cells activated with mAb to CD3 and mAb to CD28 (CD3-CD28); colors (key, top left image) indicate local point-pattern-analysis values (Getis and Franklin) ranging from low (blue) to high (red). Scale bar, 1 μm. (**b**,**c**) Quantitative analysis of Lat clustering in the cells in **a**, presented as total Lat density (**b**) and density of Lat molecules in clusters (**c**). Each symbol represents an individual cell; horizontal lines indicate the mean. $*P \leq 0.0001$ (Student's *t*-test). Data are representative of two experiments.

Because T lymphocytes do not express receptors for tetanus neurotoxin, we transfected Jurkat cells with a gene encoding the proteolytic light chain of tetanus neurotoxin or an inactive mutant (with substitution of glutamic acid for glutamine at position 234)[17]. To assess the protease activity of tetanus neurotoxin in our model, we coexpressed tetanus neurotoxin with VAMP3 (a tetanus neurotoxin–sensitive substrate) tagged at its cytosolic amino terminus with green fluorescent protein (GFP-VAMP3). This chimeric molecule was expressed at the membrane of endosomes. The active form of tetanus neurotoxin efficiently cleaved GFP-VAMP3, which led to the release of GFP into the cytosol (**Fig. 1e**). We did not observe such cleavage in T cells expressing the inactive mutant tetanus neurotoxin (**Fig. 1e**). We then measured the recruitment of Lat in Jurkat cells coexpressing Lat tagged with the red fluorescent protein mCherry (Lat-mCherry) plus active or inactive tetanus neurotoxin. Activated T cells expressing active tetanus neurotoxin did not have less recruitment of Lat microclusters than did those T cells expressing the inactive tetanus neurotoxin (**Fig. 1f**), which indicated that tetanus neurotoxin–sensitive SNARE proteins were not involved in the recruitment of Lat. Together these results indicated that VAMP7, a neurotoxin-insensitive SNARE, was involved in the recruitment of Lat-containing vesicles to TCR-activation sites.

Recruitment and clustering of Lat in cells depleted of VAMP7

To gain further insight into the role of VAMP7 in the recruitment of Lat, we used single-molecule photoactivation-localization microscopy (PALM)[10,12]. We tagged Lat with the photoactivatable protein PS-CFP2 and expressed this in Jurkat cells that we activated on coverglasses coated with mAb to CD3 and mAb to CD28 or fixed in suspension and adhered to coverslips. We applied stringent parameters for single-molecule detection so that reexcited molecules and molecules with localization precisions above 50 nm were excluded from further analysis. We used the molecular coordinates of individual Lat molecules for a distribution analysis of Lat based on the Ripley *K*-function. This allowed us not only to measure total Lat density at the cell surface in resting and activated Jurkat under conditions of normal and diminished VAMP7 expression but also to quantify Lat molecules in clusters in each condition. Silencing of VAMP7 with shRNA resulted in impaired recruitment of Lat so that we found less Lat molecules in activated Jurkat cells expressing VAMP7-specific shRNA than in those expressing control shRNA (**Fig. 2a**,**b**). Furthermore, activated Jurkat cells expressing VAMP7-specific shRNA also had significantly fewer Lat molecules in clusters than did Jurkat cells expressing control shRNA (**Fig. 2a**,**c**). These observations indicated that VAMP7 controlled the recruitment of clustered Lat from vesicular pools to TCR-activation sites.

Subsynaptic Lat vesicles do not fuse with the plasma membrane

VAMP7 can mediate the fusion and/or the anchoring and docking of vesicles with target membranes[18]. We thus investigated whether Lat vesicles docked or fused with the plasma membrane after activation via the TCR. We engineered a Lat molecule with an extracellular hemagglutinin (HA) tag that could be cleaved with tobacco etch virus (TEV) protease (HA-TEV-Lat). Univariate population comparison of cytofluorimetric HA labeling of untransfected Jurkat cells versus Jurkat cells transfected with HA-TEV-Lat (permeabilized and nonpermeabilized cells) identified significant differences between the cells (**Fig. 3a**), which indicated that HA-TEV-Lat was expressed and present at the plasma membrane of tranfected Jurkat cells. Activation on glass slides coated with activating antibodies induced recruitment to the plasma membrane of new HA-TEV-Lat microclusters (**Fig. 3b**), which indicated that the intracellular pool of chimeric Lat acted like the subvesicular pool of endogenous Lat. To prevent extracellular HA labeling, we treated the Jurkat cells expressing HA-TEV-Lat with TEV protease, which is cell impermeable. We then activated cells for 10 min or 30 min to assess whether intracellular pools of HA-TEV-Lat recruited after activation fused with the plasma membrane. Univariate population comparison of cytofluorimetric HA labeling of Jurkat cells transfected with HA-TEV-Lat at time 0 and those at 10 min and 30 min after activation (all nonpermeabilized cells) showed no significant differences between the cells (**Fig. 3c**). This indicated that the intracellular pool of HA-TEV-Lat, although brought in close proximity to the plasma membrane (**Fig. 3b**), did not fuse with it at these time points. This was not due to an intrinsic inability of the construct to fuse with the plasma membrane, because after 2 h of activation, there was more labeling of HA-TEV-Lat at the plasma membrane (**Fig. 3c**), which indicated that the newly synthesized pool of HA-TEV-Lat was able to fuse. In addition, Jurkat cells expressing HA-TEV-Lat were normally activated by mAb to CD3 and mAb to CD28, as shown by greater phosphorylation of mitogen-activated protein kinase (MAPK; **Supplementary Fig. 3**). Together these data indicated that the intracellular pools of Lat that were recruited to the site of TCR activation did not fuse with the plasma membrane.

VAMP7 decorates vesicular pools of Lat

Because VAMP7 was required for the recruitment of Lat to the site of TCR activation, we next analyzed the localization of VAMP7 relative to that of Lat in T cells. We first imaged VAMP7 and Lat in Jurkat cells that formed conjugates with Raji human B cells, left unpulsed or pulsed with the activating superantigen staphylococcus

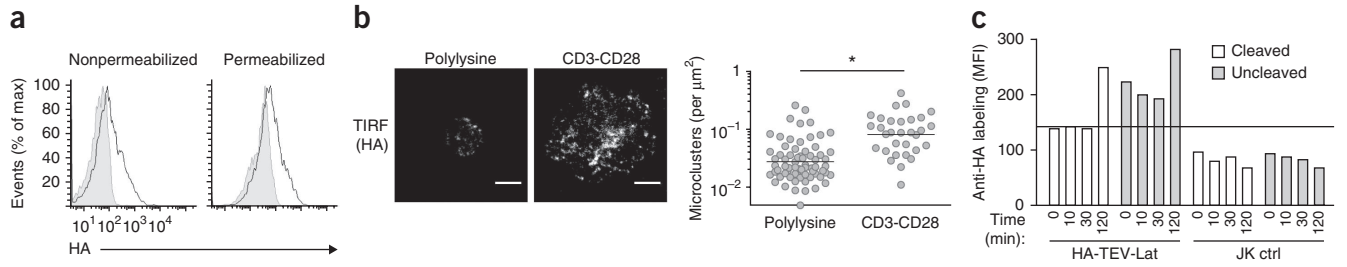

Figure 3 Subsynaptic vesicles containing Lat do not fuse with the plasma membrane. (**a**) Cytofluorimetry of the expression of HA-TEV-Lat in Jurkat cells left untransfected (gray shaded curves) or transfected to express HA-TEV-Lat (black lines) and labeled with mAb to HA, assessed before (left) or after (right) permeabilization. $P < 0.01$. (**b**) TIRF images of the recruitment of HA-TEV-Lat to the interface between coverslips coated with polylysine or with mAb to CD3 and mAb to CD28 and Jurkat cells transfected to express HA-TEV-Lat, fixed, permeabilized and stained with antibody to HA, assessed at 10 min (left), and density of HA-labeled microclusters (right) in cells as at left. Scale bars (left), 5 µm. Each symbol (right) represents an individual cell (polylysine, $n = 69$; CD3-CD28, $n = 31$); horizontal lines indicate the geometric mean. $^*P \leq 0.0001$ (Student's *t*-test). (**c**) Membrane expression of HA in untransfected control Jurkat cells (JK ctrl) or Jurkat cells transfected to express HA-TEV-Lat (HA-TEV-Lat), then left untreated (Uncleaved) or treated with TEV protease (Cleaved) and then activated for various times (horizontal axis) with mAb to CD3 and mAb to CD28 and assessed by cytofluorimetry of nonpermeabilized cells as in **a**, presented as the mean fluorescent intensity (MFI) of labeling with anti-HA. Horizontal line, HA labeling at time 0 in Jurkat cells transfected to express HA-TEV-Lat and treated with TEV protease. Data are from one experiment representative of three experiments (**a**,**c**) or represent two experiments (**b**).

enterotoxin E (SEE; **Fig. 4a**). VAMP7-labeled intracellular compartments were present around the microtubule-organizing center (maximal α-tubulin signal) in nonpolarized T cells. Those intracellular compartments were recruited toward the immunological synapse in response to SEE-pulsed APCs. 'Colabeling' showed partial localization and recruitment of Lat and VAMP7 together to the immunological synapse when T cells were forming conjugates with SEE-pulsed APCs (**Fig. 4a**; Pearson's coefficient, 0.83 ± 0.04 ($n = 16$ cells)). To analyze whether both molecules were recruited to TCR-activation sites, we incubated GFP-VAMP7–expressing Jurkat cells for 10 min on coverslips coated with poly-L-lysine or with mAb to CD3 and mAb to CD28 and imaged the recruitment of both endogenous Lat and VAMP7-GFP by TIRF microscopy. Both molecules were recruited to the activation sites (**Fig. 4b**,**c**). Further analysis showed colocalization of vesicular VAMP7-GFP and endogenous Lat in the TIRF illumination zone (Pearson's coefficient, 0.70 ± 0.12 ($n = 34$ cells)). We then dynamically imaged the recruitment of Lat and VAMP7 to the activation sites by TIRF microscopy of Jurkat cells transfected to express both Lat-mCherry and VAMP7-GFP. We placed transfected cells on glass slides coated with activating antibodies and acquired images after cell spreading.

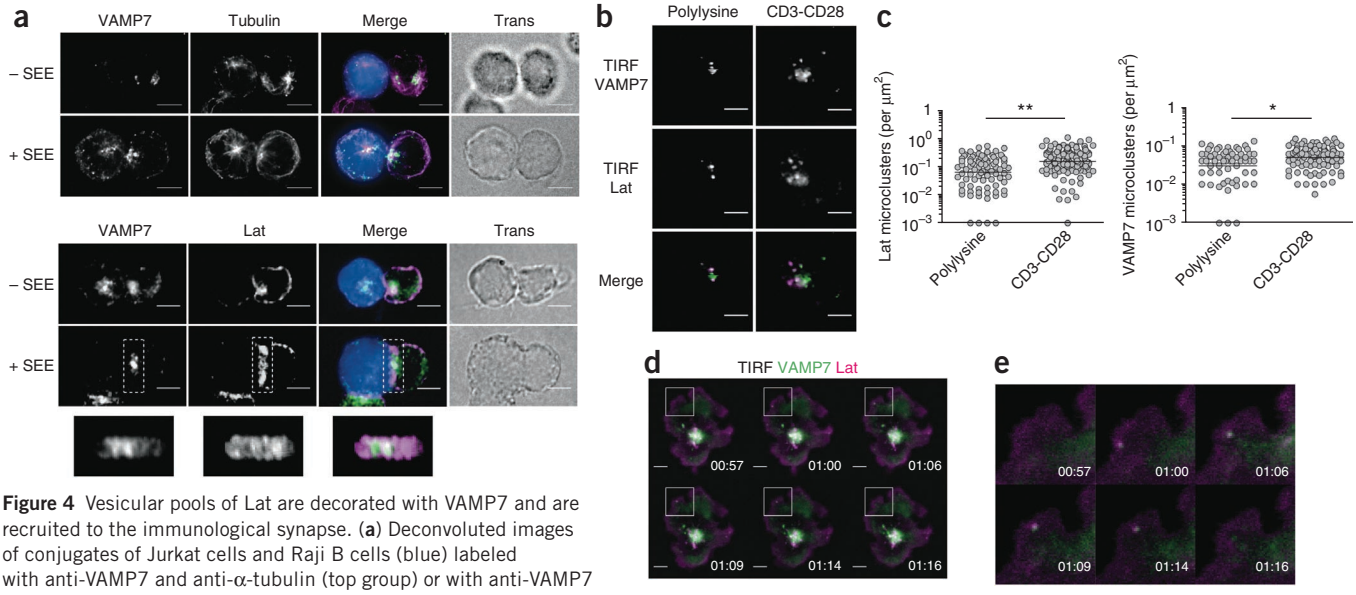

Figure 4 Vesicular pools of Lat are decorated with VAMP7 and are recruited to the immunological synapse. (**a**) Deconvoluted images of conjugates of Jurkat cells and Raji B cells (blue) labeled with anti-VAMP7 and anti-α-tubulin (top group) or with anti-VAMP7 and anti-Lat (bottom group), cultured for 30 min under resting conditions (–SEE) or activating conditions (+SEE). Trans (far right), corresponding transmission images. Below, orthogonal projection of the synaptic contact outlined above (white dashed lines). Scale bars, 5 µm. (**b**) TIRF images of the recruitment of GFP-VAMP7 and endogeneous Lat to the interface between coverslips coated with polylysine or with mAb to CD3 and mAb to CD28 and Jurkat cells expressing GFP-VAMP7 and fixed, permeabilized and stained for endogenous Lat, assessed at 10 min. (**c**) Density of microclusters containing Lat (left) or VAMP7 (right) in the cells in **b**. Each symbol represents an individual cell (polylysine and Lat, $n = 46$; polylysine and VAMP7, $n = 48$; mAb to CD3 and mAb to CD28 and Lat, $n = 63$; mAb to CD3 and mAb to CD28 and VAMP7, $n = 49$); horizontal lines indicate the geometric mean. $^*P \leq 0.01$ and $^{**}P \leq 0.0001$ (Student's *t*-test). (**d**) Still images of time-lapse TIRF microscopy of Jurkat cells transfected to express both Lat-mCherry (magenta) and GFP-VAMP7 (green), then put on glass slides coated with mAb to CD3 and mAb to CD28. Time, bottom right corners (minutes:seconds). Scale bars, 5 µm. (**e**) Enlargement of the areas outlined in **d**. Data are representative of three experiments (**a**) or two experiments (**b**,**d**,**e**) or represent two experiments (**c**).

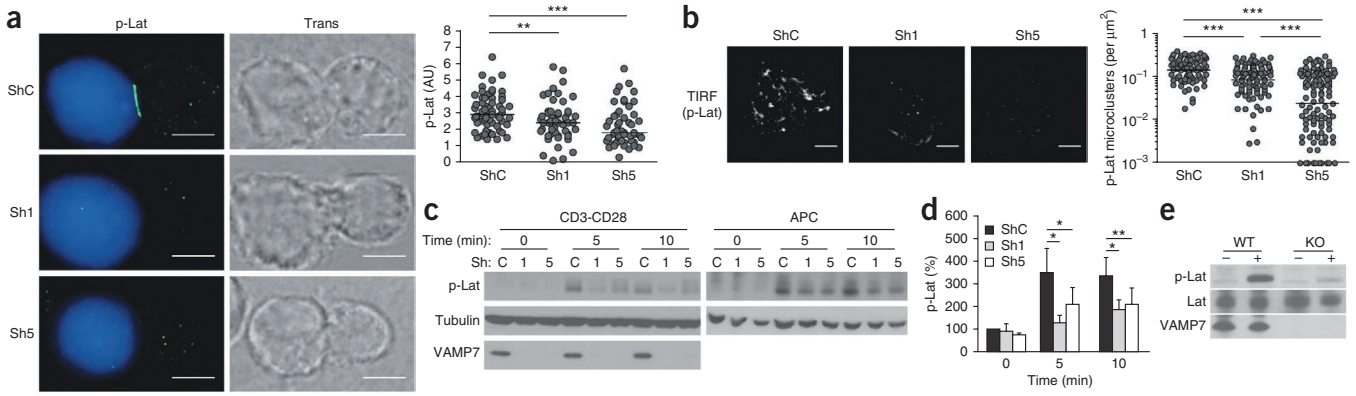

Figure 5 VAMP7 controls Lat phosphorylation after T cell activation. (**a**) Deconvoluted images of conjugates of Jurkat cells expressing control or VAMP7-specific shRNA and SEE-pulsed Raji B cells (blue) labeled with antibody to phosphorylated Lat (p-Lat), assessed at 30 min (left), and quantification of the mean fluorescence intensity of phosphorylated Lat (right), assessed on two *z* planes in a fixed region of the immunological synapse and divided by that of the entire T cell measured on the same two *z* planes (ShC, $n = 61$ cells; Sh1, $n = 55$ cells; Sh5, $n = 64$ cells). (**b**) TIRF microscopy of the recruitment of phosphorylated Lat to the interface between coverslips coated with anti-CD3 and anti-CD28 and Jurkat cells expressing control or VAMP7-specific shRNA (left), and density of microclusters containing phosphorylated Lat (right). (**c**) Immunoblot analysis of phosphorylated Lat in Jurkat cells expressing control shRNA (C) or VAMP7-specific shRNA (Sh1 (1) or Sh5 (5)), activated for various times (above blots) with anti-CD3 and anti-CD28 (CD3-CD28) or with Raji B cells and SEE (APC). (**d**) Intensity of the phosphorylated Lat signal obtained by immunoblot analysis of Jurkat cells expressing control shRNA or VAMP7-specific shRNA and activated for 0, 5 or 10 min with anti-CD3 and anti-CD28; results are normalized to tubulin and are presented relative to those of unstimulated cells expressing control shRNA. (**e**) Immunoblot analysis of CD4$^+$ T cells obtained from VAMP7-deficient mice and their VAMP-sufficient (wild-type) littermates and left unactivated (–) or activated for 4 min with mAb to CD3 and mAb to CD28 (+). Scale bars (**a**,**b**, left), 5 μm. Each symbol (**a**,**b**, right) represents an individual cell; horizontal lines indicate the geometric mean. $*P \le 0.05$, $**P \le 0.01$ and $***P \le 0.001$ (Student's *t*-test). Data represent three experiments (**a**), two experiments (**b**) or eight experiments (**d**; mean and s.e.m.) or are representative of eight experiments (**c**) or three experiments (**e**).

Activation induced the appearance of new Lat microclusters that localized together with VAMP7 at or near the plasma membrane (**Fig. 4d**,**e** and **Supplementary Video 4**). The lifetime of these microsclusters was less than 1 min (typically in the range of 10 s), with Lat clusters appearing and disappearing rapidly (**Fig. 4d**,**e** and **Supplementary Video 4**). This activity of the clusters was consistent with that of vesicles docking and undocking at the plasma membrane[12]. Together these results showed that VAMP7 was present in the vesicular pools of Lat that were recruited to TCR-activation sites.

VAMP7 controls TCR-induced phosphorylation of Lat

TCR-induced recruitment of Lat precedes and is essential for the phosphorylation of Lat[12]. We thus examined the phosphorylation of Lat in Jurkat cells in which VAMP7 was silenced by shRNA, which we activated with superantigen-pulsed APCs. There was significantly less enrichment for phosphorylated Lat at the synapse in Jurkat cells in which VAMP7 was silenced by shRNA (**Fig. 5a**). TIRF microscopy of fixed T cells incubated for 10 min on coverslips coated with activating antibodies and labeled with antibody to phosphorylated Lat also showed significantly fewer microclusters containing phosphorylated Lat in Jurkat cells and human primary T cells in which VAMP7 was silenced by shRNA (**Fig. 5b** and **Supplementary Fig. 1d**). We then checked by immunoblot analysis the phosphorylation of Lat in Jurkat cells in which VAMP7 was silenced by shRNA, followed by activation with mAb to CD3 and mAb to CD28 or with SEE-pulsed Raji B cells. In both conditions, silencing of VAMP7 by shRNA was accompanied by less phosphorylation of Lat (**Fig. 5c**,**d**). Moreover, there was also less phosphorylation of Lat in CD4$^+$ T cells obtained from VAMP7-deficient mice and activated by mAb to CD3 and mAb to CD28 than in activated CD4$^+$ T cells from their wild-type littermates (**Fig. 5e**). These results showed that VAMP7, which controlled the recruitment of the vesicular pool of Lat to TCR-activation sites, was also required for the phosphorylation of Lat after activation via the TCR.

VAMP7 controls TCR-induced activation of T cells

Because Lat has a crucial role in T cell activation, we analyzed the role of VAMP7 in TCR-induced activation of T cells. Jurkat cells and human primary T cells in which VAMP7 was silenced by shRNA and that were activated by APCs pulsed with superantigen (Raji B cells or monocyte-derived dendritic cells, respectively) had lower production of interleukin 2 (IL-2) than did cells expressing control shRNA, at all concentrations of superantigen used (**Fig. 6a**,**b**). Next, we crossed *Vamp7*$^{+/-}$ females with male OT-II mice (which have transgenic expression of a TCR specific for chicken ovalbumin (OVA) peptide of amino acids 323–339 (OVA(323–339)) in the context of I-A^b). We purified CD4$^+$ T cells from the offspring of that cross, both from male VAMP7-deficient mice (called '*Vamp7*$^{-/Y}$ OT-II' here) and from their male VAMP7-sufficient littermates (called '*Vamp7*$^{+/Y}$ OT-II' here; *Vamp7* is an X-linked gene) and activated the cells with lipopolysaccharide-stimulated dendritic cells pulsed with OVA(323–339). Expression of the activation marker CD69 at 20 h (**Fig. 6c**), the concentration of IL-2 in supernatants at 20 h (**Fig. 6d**) and proliferation at 72 h (**Fig. 6e**) were all lower in activated CD4$^+$ T cells from *Vamp7*$^{-/Y}$ OT-II mice than in activated CD4$^+$ T cells from *Vamp7*$^{+/Y}$ OT-II mice. These results indicated that VAMP7 expression was required for efficient antigenic stimulation of CD4$^+$ T cells. In contrast, stimulation with the phorbol ester PMA plus ionomycin induced similar CD69 expression and IL-2 production in CD4$^+$ T cells from *Vamp7*$^{-/Y}$ OT-II and those from *Vamp7*$^{+/Y}$ OT-II mice (**Fig. 6c**,**d**), which demonstrated that VAMP7-deficient T cells did not have intrinsic defects in signaling downstream of TCR activation. These results indicated that VAMP7 was required for TCR-induced activation of T cells.

VAMP7 controls Lat signalosome formation

To gain further insights into the mechanisms involved in the regulation of T cell activation, we next analyzed the TCR-induced

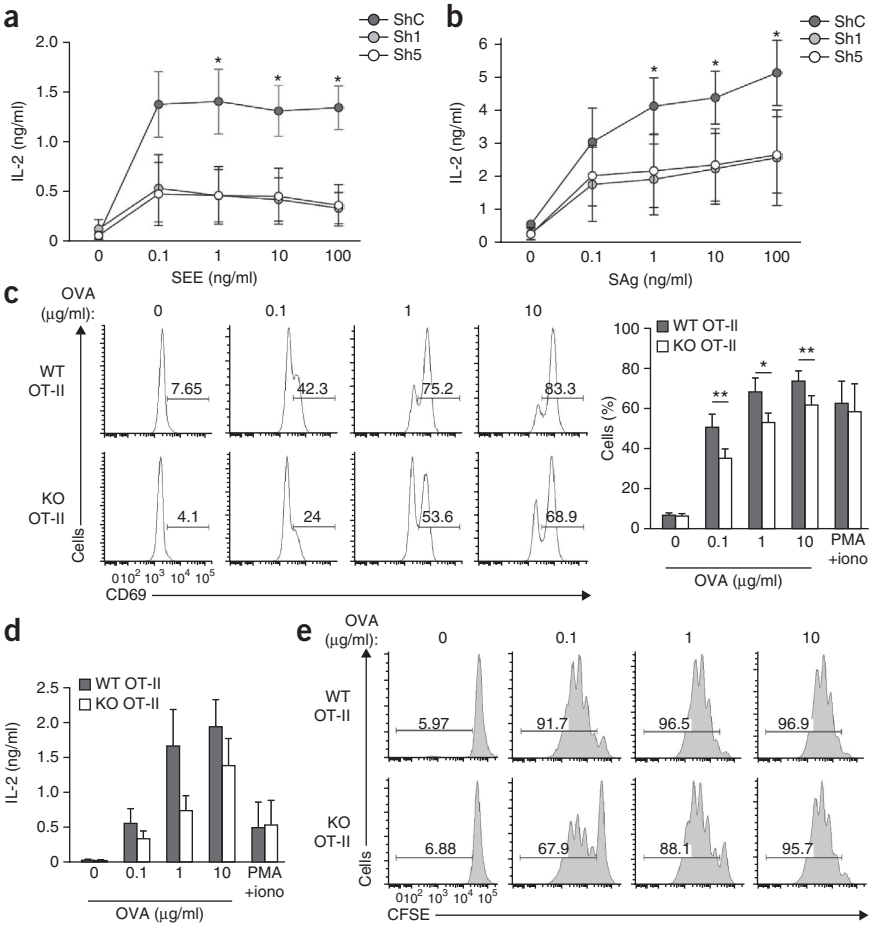

Figure 6 VAMP7 controls the TCR-induced activation of T cells. (**a**) Enzyme-linked immunosorbent assay of IL-2 in supernatants of Jurkat cells expressing control or VAMP7-specific shRNA (key) and activated for 6 h by Raji B cells pulsed with various concentrations (horizontal axis) of SEE. (**b**) IL-2 in supernatants of primary human CD4$^+$ T cells expressing control or VAMP7-specific shRNA and activated for 6 h by dendritic cells pulsed with various concentrations of the superantigens SEE, staphylococcal enterotoxin B and toxic shock syndrome toxin-1 (SAg). $^*P \leq 0.05$ (**a**,**b**), control shRNA versus VAMP7-specific shRNA (one-way analysis of variance). (**c**) Cytofluorimetry of CD69 expression in CD4$^+$ T cells obtained from *Vamp7*$^{+/Y}$ OT-II mice (WT OT-II) or *Vamp7*$^{-/Y}$ OT-II mice (KO OT-II) and activated for 20 h *in vitro* with lipopolysaccharide-treated dendritic cells pulsed with various amounts (above plots) of OVA(323–339) (left), and frequency of T cells expressing CD69 among those treated as at left or stimulated with PMA and ionomycin (PMA+iono; right). Numbers above bracketed lines (left) indicate percent CD69$^+$ T cells. $^*P \leq 0.05$ and $^{**}P \leq 0.01$ (Student's *t*-test). (**d**) IL-2 in supernatants of the cells in **c** at 20 h. (**e**) Cytofluorimetry of dilution of the cytosolic dye CFSE by the T cells in **c**, activated for 72 h. Numbers above bracketed lines indicate percent proliferating T cells. Data represent three independent experiments (**a**,**b**; mean and s.e.m.), five independent experiments (**c**,**d**; mean and s.e.m.) or are representative of four experiments (**e**).

signaling cascade. As TCR-induced phosphorylation of Lat depends on Zap70 activity, we first studied the phosphorylation of Zap70 after TCR triggering in Jurkat cells in which VAMP7 was silenced by shRNA. Quantitative immunoblot analysis of the phosphorylation of Zap70 did not show a substantial difference between T cells in which VAMP7 was silenced and control T cells in which it was not silenced (**Fig. 7a**,**b**), which demonstrated that Zap70 was normally activated. Moreover, enrichment for TCRs (**Supplementary Fig. 4c**) and for the TCR-CD3–associated ζ-chain (**Supplementary Fig. 4a**) at the immunological synapse, as well as tyrosine phosphorylation of the ζ-chain, were similar in both groups of T cells (**Supplementary Fig. 4b**), which suggested that VAMP7 was not involved in delivery of the TCR-CD3ζ complexes to the immunological synapse. We then studied the phosphorylation of phospholipase C-γ1 (PLC-γ1) and the adaptor SLP-76, which have been shown to interact with Lat[19,20]. Phosphorylation of PLC-γ1 and SLP-76 induced by mAb to CD3 and mAb to CD28 was not diminished substantially by silencing of VAMP7 with shRNA (**Fig. 7a–d**). These results suggested that TCR-induced phosphorylation of SLP-76 and PLC-γ1 was independent of the recruitment and phosphorylation of vesicular Lat. The normal tyrosine-phosphorylation of SLP-76 in T cells in which VAMP7 was silenced and in which Lat was neither recruited to the immunological synapse nor phosphorylated was in accordance with published results obtained for Lat-deficient CD4$^+$ T cells, in which phosphorylation of SLP-76 is unaffected[8]. In contrast, phosphorylation of the MAPKs Erk1 and Erk2 was significantly lower in T cells in which VAMP7 was silenced than in control T cells in which it was not silenced, as shown by immunoblot analysis (**Fig. 7a**,**e**) and flow cytometry (**Supplementary Fig. 5**).

Because Lat is a key scaffolding molecule required for the assembly of Lat signalosomes[9], we investigated whether VAMP7 controlled the formation of Lat signalosomes in T lymphocytes. We activated Jurkat cells expressing control shRNA or one of the two VAMP7-specific shRNAs with magnetic beads coated with mAb to CD3 and mAb to CD28. We retained bead-cell conjugates on a magnet and subjected them to various cycles of freezing and thawing. We then retained the bead-associated complexes on the magnet, washed them, separated them by SDS-PAGE and analyzed them by immunoblot. T cells transfected with control shRNA showed progressive enrichment for Lat and signaling molecules known to interact with Lat in the membrane fragments bound to the antibody-coated beads (**Fig. 7f**), as described before[21]. Of note, the membrane fraction bound to the antibody-coated beads also showed enrichment for VAMP7 (**Fig. 7f**), which confirmed the finding that VAMP7 was recruited together with Lat to TCR-activation sites. In contrast, Lat was not recruited to activation sites in Jurkat cells in which VAMP7 was silenced (**Fig. 7f**). Moreover, although PLC-γ1 and SLP-76 were phosphorylated in total cell lysates from T cells in which VAMP7 was silenced by shRNA (**Fig. 7a–d**), those signaling proteins were not present in membrane fragments bound to the antibody-coated beads (**Fig. 7f**). These results indicated that phosphorylation of those proteins did not depend on formation of the Lat signalosome and suggested that formation of the Lat signalosome and/or phosphorylation of Lat were (was) required for stabilization of the interaction of the signaling molecules with the TCR-CD3 complexes. As a control, we found CD3ε in signalosomes from T cells in which VAMP7 was silenced by shRNA and T cells in which it was not silenced (**Fig. 7f**), which showed that CD3 was precipitated correctly by the activating beads. Finally, we reasoned that the vesicles containing VAMP7 needed a t-SNARE partner at the site of

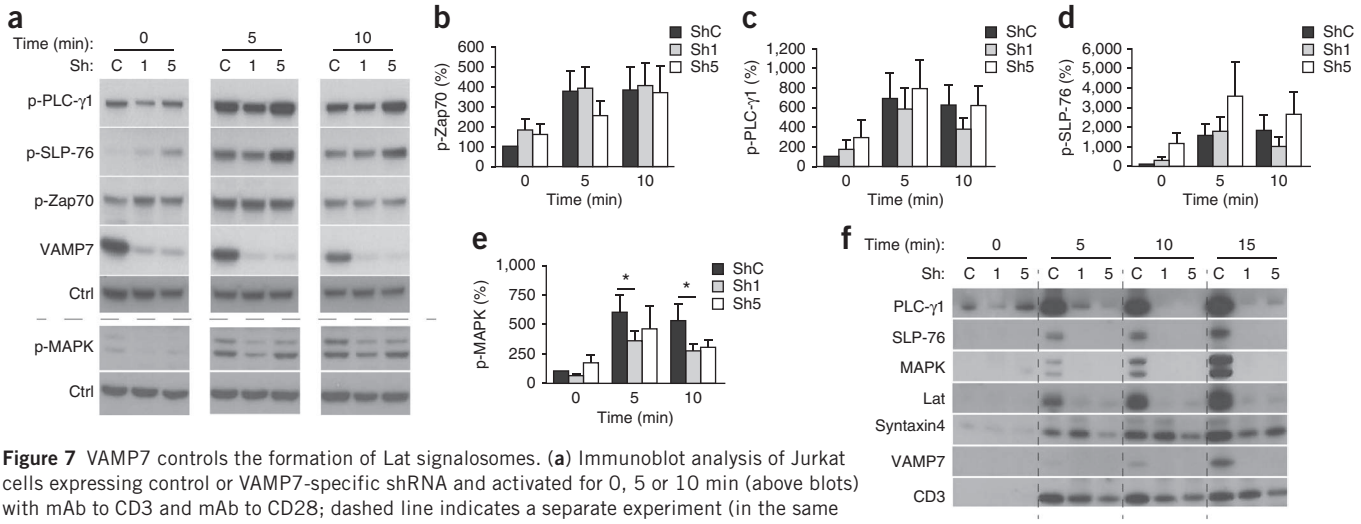

Figure 7 VAMP7 controls the formation of Lat signalosomes. (**a**) Immunoblot analysis of Jurkat cells expressing control or VAMP7-specific shRNA and activated for 0, 5 or 10 min (above blots) with mAb to CD3 and mAb to CD28; dashed line indicates a separate experiment (in the same conditions). Ctrl, loading control. (**b**–**e**) Intensity of the signals for phosphorylated Zap70 (**b**), PLC-γ1 (**c**), SLP-76 (**d**) and MAPK (**e**) measured by immunoblot analysis, normalized to tubulin and presented relative to that of unstimulated cells expressing control shRNA. $*P \leq 0.05$ (Student's *t*-test). (**f**) Immunoblot analysis of the recruitment of signaling molecules (left margin; recruitment indicated by presence of band in blot) to TCR-activation sites in Jurkat cells expressing control or VAMP7-specific shRNA, incubated for 5, 10 or 15 min with magnetic beads coated with anti-CD3 and anti-CD28 or for 15 min with magnetic beads coated with mouse IgG (0) and then lysed; proteins attached to the beads were purified by magnetic sorting. Data are representative of four to seven experiments (**a**) or three experiments (**f**) or represent seven (**b**,**e**) or four (**c**,**d**) experiments (**b**–**e**; mean and s.e.m.).

TCR recruitment. Syntaxin 4, a known t-SNARE partner of VAMP7 (ref. 22), was present at TCR-activation sites in both cells in which VAMP7 was silenced by shRNA and control cells in which it was not silenced (**Fig. 7f**), which suggested that the association of syntaxin 4 with the site of TCR activation preceded the recruitment of VAMP7. Hence, these results suggested a model in which VAMP7 controls the TCR-induced recruitment of preexisting intracellular pools of Lat, their phosphorylation and the formation of Lat signalosomes at the site of TCR activation, which facilitates T cell activation.

DISCUSSION

Here we have shown that the SNARE protein VAMP7, which is involved in the exocytosis of synaptic vesicles and granules in various cell types[18], was required for the recruitment of vesicular Lat to TCR-activation sites, for the phosphorylation of Lat and for T cell activation. This mechanism seemed to be specific for VAMP7 or at least for neurotoxin-insensitive SNARE proteins. So far, in T cells, SNARE proteins have been linked to the release of cytolytic granules from cytotoxic T cells[23] and to the efficient accumulation of recycling TCRs at the immunological synapse[24]. Our results have shown involvement of a SNARE-dependent mechanism in TCR-induced signaling, which indicates that TCR signaling involves the transport, docking and fusion of intracellular pools of signaling molecules. Similar control of receptor signaling by VAMP7 has been reported in epithelial cells in which depletion of VAMP7 impairs MAPK signaling induced by epidermal growth factor receptor[25]. Thus, VAMP7 is possibly involved in receptor signaling in several cell types, and data showing functional defects, such as phagocytosis[26] or degranulation[27–29], in VAMP7-deficient cells might need to be reinterpreted accordingly. Our study has also indicated that the signaling components proximal to the TCR are not arranged in a linear cascade. Indeed, whereas the phosphorylation of Lat depended on VAMP7 expression, the phosphorylation of PLC-γ1 and SLP-76, which in the linear-cascade model are downstream of the phosphorylation of Lat, did not depend on VAMP7. Those results are in agreement with results showing that genetic ablation of Lat in mice does not block phosphorylation of SLP-76 by Zap70 (ref. 8) and that signaling molecules downstream of the TCR are organized in functional nanoclusters[11,30,31]. Our results have also shown that formation of the Lat signalosome depended on the expression of VAMP7, which suggests that this signalosome originates from vesicular Lat rather than from the pool present at the plasma membrane[10]. However, our data do not exclude the possibility that the clustering of plasma-membrane Lat has a role in early signaling immediately after receptor engagement and before the involvement of vesicular Lat[31]. Unexpectedly, although PLC-γ1 and SLP-76 were phosphorylated in VAMP7-deficient T cells, these molecules were not present in membrane fragments bound to activating beads coated with mAb to CD3 and mAb to CD28 in T cells in which VAMP7 was silenced. These results suggest that the vesicular pool of Lat may directly retain SLP-76 and PLC-γ1 at TCR-activation sites by the formation of the Lat signalosome or indirectly by inducing cytoskeleton remodeling in the synaptic zone[4].

The absence of phosphorylation of Lat and formation of Lat signalosomes in VAMP7-deficient T cells was accompanied by defective TCR-induced production of IL-2 that fits with the known role of Lat in T cell activation[7]. This defect was more pronounced in T cells (Jurkat or primary human T cells) in which VAMP7 was acutely silenced by shRNA than in T cells from VAMP7-deficient mice. This suggested a developmental adaptation of T cells in VAMP7-deficient mice that led to compensatory mechanisms that partially masked the role of VAMP7. Compensatory mechanisms may also explain the finding that T cell development was not defective in VAMP7-deficient mice (data not shown), whereas defective T cell development has been reported for Lat-deficient mice[6].

As for the origin of the vesicular pool of Lat, Lat is present in transferrin-containing vesicles[5], which are recruited to the immunological synapse[24]. It is also ubiquitinated[32] and thus might traffic through late endocytic compartments that are also recruited to the immunological synapse[33,34]. Finally, the newly synthesized pool of Lat present in the *trans*-Golgi network, which is polarized toward the immunological synapse[35], might supply the vesicular Lat. VAMP7 is present in all those compartments[18] and thus any of those compartments may

constitute the vesicular pool of Lat recruited to the immunological synapse. As for regulation of the recruitment and phosphorylation of Lat, the vesicular pool of Lat must somehow 'meet' TCR clusters so that the associated kinases can phosphorylate the vesicle-associated Lat. Our results suggest that this does not happen in *cis*, as vesicular Lat recruited early after activation did not fuse with the plasma membrane. Instead, a *trans* mechanism may operate, involving either the transport and docking (without fusion) of Lat-containing vesicles to the plasma membrane or the docking and-or fusion of endosomes containing TCR-CD3–immunoreceptor tyrosine-based activation motif–kinase complexes with the Lat-containing vesicles. Indeed, engagement of the TCR induces the internalization of TCR-CD3 complexes[36]. Thus, part of the TCR-induced signaling cascade may take place in endocytic compartments, as shown for signaling induced by the B cell antigen receptor[37]. In the first hypothesis, VAMP7 would control transport and docking without the fusion of Lat-containing vesicles with the plasma membrane, which would allow Lat phosphorylation in *trans*. That is compatible with the biochemical properties of VAMP7, which contains an autoinhibitory Longin domain[18] and has a low fusion efficiency. VAMP7 may also control Lat transport through its involvement in the formation of a kinesin-containing network that allows the transport of the VAMP7-containing vesicles on microtubules from the cell center to the periphery[38]. That scenario is in agreement with our data demonstrating that VAMP7 and intracellular Lat vesicles were gathered around the microtubule-organizing center and were recruited to the immunological synapse together with the microtubule-organizing center and with published results showing that microtubules control propagation of the activation signal from the TCR to Lat[39]. In the second hypothesis, VAMP7 might control the transport, docking and fusion of Lat-containing vesicles with endocytic compartments containing TCR-CD3–immunoreceptor tyrosine-based activation motif–kinase complexes and thus allow Lat phosphorylation.

TCR triggering must reorganize the membrane (whether the plasma membrane or endocytic membranes) to allow subsynaptic recruitment and docking. Such 'preconditioning' might involve the recruitment of VAMP7 partners such as syntaxins and SNAP proteins that allow the formation of SNARE complexes. Indeed, syntaxin 4 and SNAP23 are recruited to the immunological synapse[24,40], and our results have shown the presence of that syntaxin 4 in TCR-activation sites. Preconditioning of the plasma membrane might also involve remodeling of the actin cortex to facilitate the apposition and/or fusion of membranes. Indeed, actin dynamics regulate TCR-induced signaling by controlling the dynamic movement of microclusters containing signaling molecules[31,41,42]. Actin remodeling is also involved in regulating the fusion of vesicles and granules in many cell types, including T cells[43] and natural killer cells[44,45]. Finally, TCR-induced actin remodeling exerts forces[46] that might facilitate close contact between membrane compartments containing signaling molecules.

In conclusion, our data contribute to the understanding of how information is propagated through the TCR signaling network in time and space. We have demonstrated that the molecular machinery involved in transport and docking of vesicular pools of Lat with TCR-activation sites is a key regulatory element. Better understanding of how the spatio-temporal relationship between TCR and Lat operates at the molecular level will require comprehensive analysis of the composition of the subsynaptic vesicles containing Lat and the innovative application of high-resolution microscopy.

METHODS

Methods and any associated references are available in the online version of the paper.

Note: Supplementary information is available in the online version of the paper.

ACKNOWLEDGMENTS

We thank A.-M. Lennon and S. Amigorena for discussions; and P. Pierobon, V. Fraisier, P. Paul-Gilloteaux, L. Sengmanivong and the Nikon Imaging Centre at Institut Curie (Centre National de la Recherche Scientifique) for technical assistance with microscopy and image analysis. Supported by Fondation pour la Recherche Médicale (P.L. and K.C., and T.G.'s group), la Ligue contre le Cancer (J.-M.C. and A.B.), DC-Biol Labex (C.H.'s group), Institut National de la Santé et de la Recherche Médicale (T.G.'s group) and the Mairie de Paris Medical Research and Health Program (T.G.'s group).

AUTHOR CONTRIBUTIONS

P.L. designed, did and analyzed three-dimensional microscopy, TIRF microscopy and biochemistry experiments, and prepared the manuscript; D.J.W. designed, did and analyzed PALM experiments and revised the manuscript; J.-M.C. did and analyzed experiments with mouse T cells; S.D. designed vectors for and did mice genotyping; K.C. and A.B. designed and analyzed three-dimensional microscopy experiments; L.D. and T.G. provided VAMP7-deficient mice and tools; K.G. designed PALM experiments and assisted with manuscript preparation; T.G. designed VAMP7-deficient mice, discussed the results and revised the manuscript; and C.H. conceived of the study, did biochemistry experiments and prepared manuscript.

COMPETING FINANCIAL INTERESTS

The authors declare no competing financial interests.

1. Weiss, A. & Littman, D.R. Signal transduction by lymphocyte antigen receptors. *Cell* **76**, 263–274 (1994).
2. Zhang, W., Trible, R.P. & Samelson, L.E. LAT palmitoylation: its essential role in membrane microdomain targeting and tyrosine phosphorylation during T cell activation. *Immunity* **9**, 239–246 (1998).
3. Rudd, C.E. Adaptors and molecular scaffolds in immune cell signaling. *Cell* **96**, 5–8 (1999).
4. Bunnell, S.C., Kapoor, V., Trible, R.P., Zhang, W. & Samelson, L.E. Dynamic actin polymerization drives T cell receptor-induced spreading: a role for the signal transduction adaptor LAT. *Immunity* **14**, 315–329 (2001).
5. Bonello, G. *et al.* Dynamic recruitment of the adaptor protein LAT: LAT exists in two distinct intracellular pools and controls its own recruitment. *J. Cell Sci.* **117**, 1009–1016 (2004).
6. Zhang, W. *et al.* Essential role of LAT in T cell development. *Immunity* **10**, 323–332 (1999).
7. Zhang, W., Sloan-Lancaster, J., Kitchen, J., Trible, R.P. & Samelson, L.E. LAT: the ZAP-70 tyrosine kinase substrate that links T cell receptor to cellular activation. *Cell* **92**, 83–92 (1998).
8. Mingueneau, M. *et al.* Loss of the LAT adaptor converts antigen-responsive T cells into pathogenic effectors that function independently of the T cell receptor. *Immunity* **31**, 197–208 (2009).
9. Roncagalli, R. *et al.* Lymphoproliferative disorders involving T helper effector cells with defective LAT signalosomes. *Semin. Immunopathol.* **32**, 117–125 (2010).
10. Lillemeier, B.F. *et al.* TCR and Lat are expressed on separate protein islands on T cell membranes and concatenate during activation. *Nat. Immunol.* **11**, 90–96 (2010).
11. Purbhoo, M.A. *et al.* Dynamics of subsynaptic vesicles and surface microclusters at the immunological synapse. *Sci. Signal.* **3**, ra36 (2010).
12. Williamson, D.J. *et al.* Pre-existing clusters of the adaptor Lat do not participate in early T cell signaling events. *Nat. Immunol.* **12**, 655–662 (2011).
13. Südhof, T.C. The synaptic vesicle cycle revisited. *Neuron* **28**, 317–320 (2000).
14. Risselada, H.J. & Grubmuller, H. How SNARE molecules mediate membrane fusion: recent insights from molecular simulations. *Curr. Opin. Struct. Biol.* **22**, 187–196 (2012).
15. Proux-Gillardeaux, V., Rudge, R. & Galli, T. The tetanus neurotoxin-sensitive and insensitive routes to and from the plasma membrane: fast and slow pathways? *Traffic* **6**, 366–373 (2005).
16. Danglot, L. *et al.* Absence of TI-VAMP/Vamp7 leads to increased anxiety in mice. *J. Neurosci.* **32**, 1962–1968 (2012).
17. McMahon, H.T. *et al.* Cellubrevin is a ubiquitous tetanus-toxin substrate homologous to a putative synaptic vesicle fusion protein. *Nature* **364**, 346–349 (1993).
18. Chaineau, M., Danglot, L. & Galli, T. Multiple roles of the vesicular-SNARE TI-VAMP in post-Golgi and endosomal trafficking. *FEBS Lett.* **583**, 3817–3826 (2009).
19. Zhang, W. *et al.* Association of Grb2, Gads, and phospholipase C-γ1 with phosphorylated LAT tyrosine residues. Effect of LAT tyrosine mutations on T cell angigen receptor-mediated signaling. *J. Biol. Chem.* **275**, 23355–23361 (2000).
20. Asada, H. *et al.* Grf40, A novel Grb2 family member, is involved in T cell signaling through interaction with SLP-76 and LAT. *J. Exp. Med.* **189**, 1383–1390 (1999).

21. Harder, T. & Kuhn, M. Selective accumulation of raft-associated membrane protein LAT in T cell receptor signaling assemblies. *J. Cell Biol.* **151**, 199–208 (2000).
22. Rao, S.K., Huynh, C., Proux-Gillardeaux, V., Galli, T. & Andrews, N.W. Identification of SNAREs involved in synaptotagmin VII-regulated lysosomal exocytosis. *J. Biol. Chem.* **279**, 20471–20479 (2004).
23. Holt, O.J., Gallo, F. & Griffiths, G.M. Regulating secretory lysosomes. *J. Biochem.* **140**, 7–12 (2006).
24. Das, V. *et al.* Activation-induced polarized recycling targets T cell antigen receptors to the immunological synapse; involvement of SNARE complexes. *Immunity* **20**, 577–588 (2004).
25. Danglot, L. *et al.* Role of TI-VAMP and CD82 in EGFR cell-surface dynamics and signaling. *J. Cell Sci.* **123**, 723–735 (2010).
26. Braun, V. *et al.* TI-VAMP/VAMP7 is required for optimal phagocytosis of opsonised particles in macrophages. *EMBO J.* **23**, 4166–4176 (2004).
27. Mollinedo, F. *et al.* Combinatorial SNARE complexes modulate the secretion of cytoplasmic granules in human neutrophils. *J. Immunol.* **177**, 2831–2841 (2006).
28. Sander, L.E. *et al.* Vesicle associated membrane protein (VAMP)-7 and VAMP-8, but not VAMP-2 or VAMP-3, are required for activation-induced degranulation of mature human mast cells. *Eur. J. Immunol.* **38**, 855–863 (2008).
29. Marcet-Palacios, M. *et al.* Vesicle-associated membrane protein 7 (VAMP-7) is essential for target cell killing in a natural killer cell line. *Biochem. Biophys. Res. Commun.* **366**, 617–623 (2008).
30. Douglass, A.D. & Vale, R.D. Single-molecule microscopy reveals plasma membrane microdomains created by protein-protein networks that exclude or trap signaling molecules in T cells. *Cell* **121**, 937–950 (2005).
31. Sherman, E. *et al.* Functional nanoscale organization of signaling molecules downstream of the T cell antigen receptor. *Immunity* **35**, 705–720 (2011).
32. Balagopalan, L. *et al.* c-Cbl-mediated regulation of LAT-nucleated signaling complexes. *Mol. Cell Biol.* **27**, 8622–8636 (2007).
33. Vardhana, S., Choudhuri, K., Varma, R. & Dustin, M.L. Essential role of ubiquitin and TSG101 protein in formation and function of the central supramolecular activation cluster. *Immunity* **32**, 531–540 (2010).
34. Alonso, R. *et al.* Diacylglycerol kinase α regulates the formation and polarisation of mature multivesicular bodies involved in the secretion of Fas ligand-containing exosomes in T lymphocytes. *Cell Death Differ.* **18**, 1161–1173 (2011).
35. Kupfer, A., Dennert, G. & Singer, S.J. Polarization of the Golgi apparatus and the microtubule-organizing center within cloned natural killer cells bound to their targets. *Proc. Natl. Acad. Sci. USA* **80**, 7224–7228 (1983).
36. Alcover, A. & Alarcon, B. Internalization and intracellular fate of TCR-CD3 complexes. *Crit. Rev. Immunol.* [In Process Citation] **20**, 325–346 (2000).
37. Chaturvedi, A., Martz, R., Dorward, D., Waisberg, M. & Pierce, S.K. Endocytosed BCRs sequentially regulate MAPK and Akt signaling pathways from intracellular compartments. *Nat. Immunol.* **12**, 1119–1126 (2011).
38. Burgo, A. *et al.* A Molecular network for the transport of the TI-VAMP/VAMP7 vesicles from cell center to periphery. *Dev. Cell* **23**, 166–180 (2012).
39. Martín-Cófreces, N.B. *et al.* End-binding protein 1 controls signal propagation from the T cell receptor. *EMBO J.* **31**, 4140–4152 (2012).
40. Antón, O.M., Andres-Delgado, L., Reglero-Real, N., Batista, A. & Alonso, M.A. MAL protein controls protein sorting at the supramolecular activation cluster of human T lymphocytes. *J. Immunol.* **186**, 6345–6356 (2011).
41. Varma, R., Campi, G., Yokosuka, T., Saito, T. & Dustin, M.L. T cell receptor-proximal signals are sustained in peripheral microclusters and terminated in the central supramolecular activation cluster. *Immunity* **25**, 117–127 (2006).
42. Babich, A. *et al.* F-actin polymerization and retrograde flow drive sustained PLCgamma1 signaling during T cell activation. *J. Cell Biol.* **197**, 775–787 (2012).
43. Chemin, K. *et al.* Cytokine secretion by $CD4^+$ T cells at the immunological synapse requires Cdc42-dependent local actin remodeling but not microtubule organizing center polarity. *J. Immunol.* **189**, 2159–2168 (2012).
44. Rak, G.D., Mace, E.M., Banerjee, P.P., Svitkina, T. & Orange, J.S. Natural killer cell lytic granule secretion occurs through a pervasive actin network at the immune synapse. *PLoS Biol.* **9**, e1001151 (2011).
45. Brown, A.C. *et al.* Remodelling of cortical actin where lytic granules dock at natural killer cell immune synapses revealed by super-resolution microscopy. *PLoS Biol.* **9**, e1001152 (2011).
46. Husson, J., Chemin, K., Bohineust, A., Hivroz, C. & Henry, N. Force generation upon T cell receptor engagement. *PLoS ONE* **6**, e19680 (2011).

ONLINE METHODS

Cells, mice and reagents. Raji B cells, Jurkat cells, Jurkat ζ-GFP cells (clone 2B5[47]) and Jurkat Lat-GFP cells were cultured as described[47]. Human primary CD4+ T cells were purified by negative selection (130-091-155, Miltenyi Biotec) as described[43]. Human dendritic cells were generated from monocytes of healthy donors as described[43]. This study was conducted according to the Helsinki Declaration, with informed consent obtained from the blood donors, as requested by the Etablissement Français du Sang. VAMP7-deficient mice[16] were crossed to C57BL/6 wild-type mice (ten generations) and to OT-II mice. Male VAMP7-deficient mice 8–12 weeks of age were compared with their male wild-type littermates (controls). Experiments on animals were done in accordance with the guidelines of the French Veterinary Department. Mouse CD4+ T cells were purified from spleen and peripheral lymph nodes through negative selection (130-095-248; Miltenyi Biotec) with an average purity of 90%. Jurkat cells and primary human CD4+ T cells were activated with anti-CD3ε (OKT3; 16-0037-85; eBioscience) and anti-CD28 (CD28.2; 302914; BioLegend). Mouse CD4+ T cells were activated with anti–mouse CD3ε (145-2C11; 553057; BD Pharmingen) and anti–mouse CD28 (37.51; 553294; BD Pharmingen). SEE, staphylococcal enterotoxin B and toxic shock syndrome toxin-1 were from Toxin Technology; OVA peptide of amino acids 323–339 (C1303) was from PolyPeptide. Lipopolysaccharide and TEV protease were from Sigma-Aldrich.

Production of lentiviral stocks and infection of Jurkat cells. Replication-defective lentivirus particles pseudotyped with the envelope G protein of vesicular stomatitis virus were produced in HEK293T cells as described[43]. These particles contained the plasmid pLKO.1-puro containing VAMP7-specific short hairpin RNA (MISSION shRNA TRCN0000059888 (sh1) or TRCN0000059892 (sh5); Sigma) or nontargeting control shRNA (MISSION shRNA SHC002; Sigma). Supernatants of HEK293T cells were collected 48 h after transfection and were spun in an ultracentrifuge (120,000*g* for 90 min). Jurkat cells were infected with concentrated virus, then puromycin (2 μg/ml) was added 24 h later and infected cells were used 96 h later.

Primary human CD4+ T cells were activated in 96-well plates coated with anti-CD3 (2.5 μg/ml) in the presence of soluble anti-CD28 (2.5 μg/ml) and recombinant IL-2 (20 U/ml). Concentrated virus was added 24 h later. Cells were washed and then put in fresh medium with IL-2 (20 U/ml) and puromycin (2.5 μg/ml) 48 h later and used 72 h later.

Antibodies. The following primary antibodies were used: antibody to Lat phosphorylated at Tyr191 (3584), antibody to Zap70 phosphorylated at Tyr319 (2701), antibody to PLC-γ1 phosphorylated at Tyr783 (2821), anti-PLC-γ1 (2822), anti-ERK1-2 (4695), anti-SLP-76 (4958) and antibody to Erk1/2 phosphorylated at Thr202 and Tyr204 (9106; all from Cell Signaling Technology); antibody to SLP-76 phosphorylated at Tyr128 (558367), anti–syntaxin 4 (610439), anti–human CD3ε (555333), anti–mouse CD3ε (553066), anti-CD4 (555346), anti-CD28 (553294) and anti-CD69 (551113; all from BD Pharmingen); anti-VAMP7 (from T.G.), mAb to Lat (IC63341A; R&D Systems); anti-α-tubulin (MCA77G; Serotec); polyclonal anti-Lat (06-807) and antibody to Lat phosphorylated at Tyr191 (07-278; both from Upstate Technology); anti-tubulin (for immunoblot analysis; CP06; Calbiochem); 'pan' antibody to human TCRαβ (A39499; Beckman Coulter); phycoerythrin-conjugated mAb to HA (130-092-257; Miltenyi Biotech); and rabbit polyclonal anti-HA (H 6908; Sigma).

Plasmids and transfection. Mammalian expression vectors encoding the chimeric GFP-VAMP7 have been described[48]. The cDNA encoding human Lat variant 2 was subcloned into the pEGFP-N1 or pmCherry-N1 vector (Clontech). The HA-TEV-Lat construct was obtained by amplification of cDNA Lat variant 2 with the following oligonucleotides: forward, 5′-**GCCACC**ATGGGA**TACCCATACGACGTCCCAGACTACGCT**gactacgacatcccacccacc**GAAAACCTGTATTTTCAGGGC**ggaggaggaagtggaggaggagga**GAGGAGGCCATCCTGGTC**-3′ (lower case, spacers; bolding as follows: first, Kozak sequence; second, HA tag; third, TEV-recognition sequence; fourth, sequence encoding the Lat amino terminus without ATG), and reverse, 5′-TCAGTTCAGCTCCTGCAG-3′.

A second round of PCR of that first PCR product was used to introduce HindIII and XhoI restriction sites. The amplification product was subcloned in a pCDNA3.1 zeocin vector (Life Technologies). Jurkat cells were transfected by electroporation. Stable cell lines expressing Lat-GFP or HA-TEV-Lat were selected with 1 mg/ml of G418 or 250 μg/ml of zeocin (Life Technologies), respectively.

Cytofluorimetry. For surface analysis by flow cytometry, antibodies were diluted in 0.1% BSA in PBS; intracellular staining was done according to the manufacturer's protocol (Cytofix/Cytoperm; BD Pharmingen). Samples were acquired on a MACSQuant (Miltenyi Biotec) or FACSCalibur (Becton Dickinson). Data were analyzed with FlowJo software (TreeStar).

Biochemistry. Jurkat cells (1×10^6/ml) were activated for the appropriate time with anti-CD3 (125 ng/ml) and anti-CD28 (250 ng/ml) in a volume of 1 ml. Alternatively, 5×10^5 Raji B cells were added to 1 ml of Jukat T cells, and SEE (100 ng/ml) was added for the appropriate time. For mouse CD4+ primary T cells, cells (5×10^7 per ml) were activated for 4 min with anti-CD3 and anti-CD28 (50 μg/ml each) in a volume of 100 μl. Cells were washed in cold PBS and lysed in (50 mM Tris, pH 8, 150 mM NaCl, 1.5 mM $MgCl_2$, 1% glycerol, 1% TritonX-100 and 0.5 mM EDTA, pH 8) supplemented with 1 mM Na_3OV_4, 5 mM NaF and 1× cOmplete, Mini, EDTA-free Protease Inhibitor Cocktail Tablet (11-836-170-001; Roche). Post-nuclear lysates were resolved by SDS-PAGE (Novex protein gels; Invitrogen) and were transferred to membranes (Immunblot PVDF membranes; Bio-Rad).

Purification of signalosomes. Jurkat cells (5×10^6) were resuspended in 200 μl of RPMI medium, and magnetic beads (1×10^7) coated with anti-CD3 and anti-CD28 (111.31; Life Technologies) or mouse IgG (110.33; Life Technologies) were added in a volume of 100 μl. Beads were incubated with T cells for the appropriate time. Activation was stopped with the addition of 500 μl cold PBS, and 80 μl (1/10) of total proteins were collected as 'input' and lysed as described above ('Biochemistry' subsection). Bead-cell conjugates were then magnetically restrained, resuspended in 500 μl of 'freeze-thaw' buffer (600 mM KCl, 20 mM Tris, pH 7.4 and 20% glycerol) supplemented with 1 mM Na_3OV_4, 5 mM NaF and 1× cOmplete, Mini, EDTA-free Protease Inhibitor Cocktail Tablet (11-836-170-001; Roche). Samples were submitted to seven cycles of freezing and thawing. After the final cycle, 20 μl benzonase (70664-3; Novagen) was added, followed by incubation for 10 min at room temperature. Samples were magnetically restrained to purify the bead-attached proteins and then were washed five times in the supplemented 'freeze-thaw' buffer described above. Bead-associated proteins were separated by SDS-PAGE and analyzed by immunoblot.

Three-dimensional and TIRF microscopy. Jurkat cells and human primary CD4+ T cells (1.5×10^5) were incubated for 10 min at room temperature on slides precoated with 0.02% poly-L-lysine alone or followed by incubation overnight at 4 °C with anti-CD3 and anti-CD28 (10 μg/ml). Alternatively, 1.5×10^5 Raji B cells were stained with 50 μM CellTracker Blue CMCA (7-amino-4-chloromethylcoumarin; C2110; Life Technologies), then were left unloaded or loaded with SEE (100 ng/ml) and were incubated for 30 min on slides precoated with 0.02% poly-L-lysine; 1.5×10^5 Jurkat cells were added, followed by incubation for 30 min at room temperature. For mouse primary CD4+ T cells, 5×10^5 cells were incubated on slides precoated with 0.02% poly-L-lysine alone or followed by incubation overnight at 4 °C with anti-CD3 and anti-CD28 (10 μg/ml). Cells were fixed in 4% paraformaldehyde in PBS. For staining of VAMP7, cells were made permeable for 4 min in 0.1% Triton in PBS and were washed three times in PBS, then nonspecific binding was blocked by incubation for 30 min in 0.25% coldwater fish gelatin (G7765; Sigma) in PBS and cells were incubated overnight at 4 °C or 45 min at room temperature, respectively, with primary and secondary antibodies diluted in 0.125% fish gelatin in PBS. For all other antibodies, cells were treated as published[43]. Coverslips were mounted onto glass slides with Fluoromount G (Southern Biotechnology Associates). Three-dimensional images were acquired with a wide-field Eclipse 90i Upright Microscope (Nikon) equipped for image deconvolution. Images were acquired with a 100× Plan Apo violet-corrected oil-immersion objective (numerical aperture, 1.4) and a highly sensitive cooled interlined charge-coupled device camera (Roper CoolSnap HQ2). Z-positioning was accomplished by a piezoelectric motor (linear variable

doi:10.1038/ni.2609

differential transformer; Physik Instrument), and a *z*-series of images was obtained every 0.2 µm. Alternatively, images were acquired with a scanning confocal microscope with Nipkow disk mounted on a TiE Nikon microscope (Yokogawa CSUX1 spinning-disk head). The system was equipped with an APO violet-corrected 60× oil-immersion objective with a numerical aperture of 1.40, laser illumination (405 nm and 50 mW; 491 nm and 100 mW; and 561 nm and 100 mW) and a coolSnap HQ2 Roper camera. A Nikon TiE microscope equipped with a 100× APO TIRF objective with numerical aperture of 1.45 and an electron-multiplying charge-coupled device camera (Roper Scientific) were used for TIRF microscopy of fixed and live cells (at 37 °C for live cells). Metamorph software was used for all acquisitions.

PALM imaging. Jurkat cells expressing wild-type Lat fused to PS-CFP2 (a derivative of the cyan-to-green photoswitchable cyan fluorescent protein PS-CFP) were activated on coverslips coated with anti-CD3 and anti-CD28; for this, cells were allowed to settle on the activating surface for 10 min at 37 °C. Cells were fixed with 4% paraformaldehyde in PBS and were made permeable with lysolecithin (100 µg/ml; L5254; Sigma). Resting Jurkat cells were first fixed in suspension and were then allowed to settle onto nonactivating coverglass surfaces coated with poly-L-lysine (P8920; Sigma). PALM images were acquired on a TIRF microscope (ELYRA; Zeiss) with a 100× oil-immersion objective with a numerical aperture of 1.46. Photoconversion of PS-CFP2 was achieved with 8 µW of 405-nm laser irradiation, and green-converted PS-CFP2 was imaged with 18 mW of 488-nm light. A total of 1.5×10^4 to 2.0×10^4 images were acquired per sample with a cooled, electron-multiplying charge-coupled device camera (iXon DU-897D; Andor) with an exposure time of 40 ms. Recorded images were processed with Zeiss ZEN software as described[49]. Sample drift was corrected to surface-immobilized 100-nm colloidal gold beads (BBInternational) placed on the coverglass.

Image analysis and treatment. For quantification of the recruitment of proteins to the immunological synapse, three-dimensional images were subjected to deconvolution as described[43]. The mean fluorescence intensity (MFI) of the signal, on two *z*-planes, in a fixed region of the immunological synapse was divided by the MFI in the T cell measured on the same two *z*-planes. For analysis of the recruitment of TCR to the immunological synapse (**Supplementary Fig. 5c**), the MFI of a TCR in a fixed region of the synapse was divided by the MFI measured in three regions outside of the synapse. These values were calculated on two intermediate confocal planes, then were averaged and plotted. For quantification of microclusters by TIRFM, a 'macro' compatible with ImageJ analysis software was used (available on request). For analysis of PALM images, two-dimensional molecular coordinates were cropped into nonoverlapping regions 3 × 3 µm in area, and events with localization precision worse than 50 nm discarded. For the construction of cluster maps, local analogue of Ripley's *K*-analysis was done as described[49] in which the value of *L(r)* was calculated for each point at a specific spatial scale (here, $r = 50$ nm). From the computed *L(50)* values for all molecules in a region, a quantitative, pseudocolored cluster map was then interpolated using the MATLAB v4 interpolation algorithm on a 10-nm resolution grid. Molecules in a region were assigned threshold at an *L(50)* value of 90 (approximately 25% of each region's maximum *L(50)* value) to identify which molecules were in clusters or not, as described[12,49]. Raw images were used for all quantifications. For image visualization, images were subjected to background subtraction (TIRF) or brightness contrast was adjusted (three images) with ImageJ software. Equal amounts of adjustment were used for all experimental groups (all three shRNAs).

Activation of primary CD4$^+$ T cells from VAMP7-deficient mice. Purified mouse CD4$^+$ T cells (1×10^7 cells per ml) were stained for 4 min at room temperature with 5 µM CFSE (carboxyfluorescein diacetate succinimidyl ester) in PBS and were washed extensively. Dendritic cells derived from the bone marrow of C57BL/6 mice as described[50] were activated overnight with lipopolysaccharide (100 ng/ml), and 2×10^5 cells were plated in triplicate in 96-well (flat-bottomed) plates. Dendritic cells were loaded for 2 h with the appropriate concentration of OVA(323–339) peptide and then washed extensively, and 1×10^5 CD4$^+$ T cells were added. Supernatants were collected and then CD69 expression was analyzed after 20 h and CFSE dilution was analyzed at 72 h.

IL-2 secretion. Jurkat cells (1×10^5) were activated with Raji cells (5×10^4) loaded with the appropriate concentration of SEE. Primary CD4$^+$ T cells were subjected to gradient centrifugation for the removal of uninfected dead cells. Infected primary CD4$^+$ T cells (1×10^5) were activated with dendritic cells (5×10^4) loaded with the appropriate concentration of SEE, staphylococcal enterotoxin B and toxic shock syndrome toxin-1. Supernatants were collected after 6 h. IL-2 was measured in the supernatants of human T cells and mouse CD4$^+$ T cells by enzyme-linked immunosorbent assay (555190 (BD) and 88-7024 (eBioscience), respectively).

Statistical analysis. PRISM software was used for statistical analysis. An unpaired Student's *t*-test was used for all microscopy analysis; a paired Student's *t* test or analysis of variance was used for all other experiments.

47. Blanchard, N., Di Bartolo, V. & Hivroz, C. In the immune synapse, ZAP-70 controls T cell polarization and recruitment of signaling proteins but not formation of the synaptic pattern. *Immunity* **17**, 389–399 (2002).
48. Martinez-Arca, S., Alberts, P., Zahraoui, A., Louvard, D. & Galli, T. Role of tetanus neurotoxin insensitive vesicle-associated membrane protein (TI-VAMP) in vesicular transport mediating neurite outgrowth. *J. Cell Biol.* **149**, 889–900 (2000).
49. Owen, D.M. *et al.* PALM imaging and cluster analysis of protein heterogeneity at the cell surface. *J. Biophotonics* **3**, 446–454 (2010).
50. Benvenuti, F. *et al.* Dendritic cell maturation controls adhesion, synapse formation, and the duration of the interactions with naive T lymphocytes. *J. Immunol.* **172**, 292–301 (2004).

Supplementary material

VAMP7 controls T cell activation by regulating recruitment and phosphorylation of vesicular Lat to the TCR activation sites.

Paola Larghi, David J Williamson, Jean-Marie Carpier, Stéphanie Dogniaux, Karine Chemin, Armelle Bohineust, Lydia Danglot, Katharina Gaus, Thierry Galli & Claire Hivroz.

Nature Immunology doi:10.1038/ni.2609

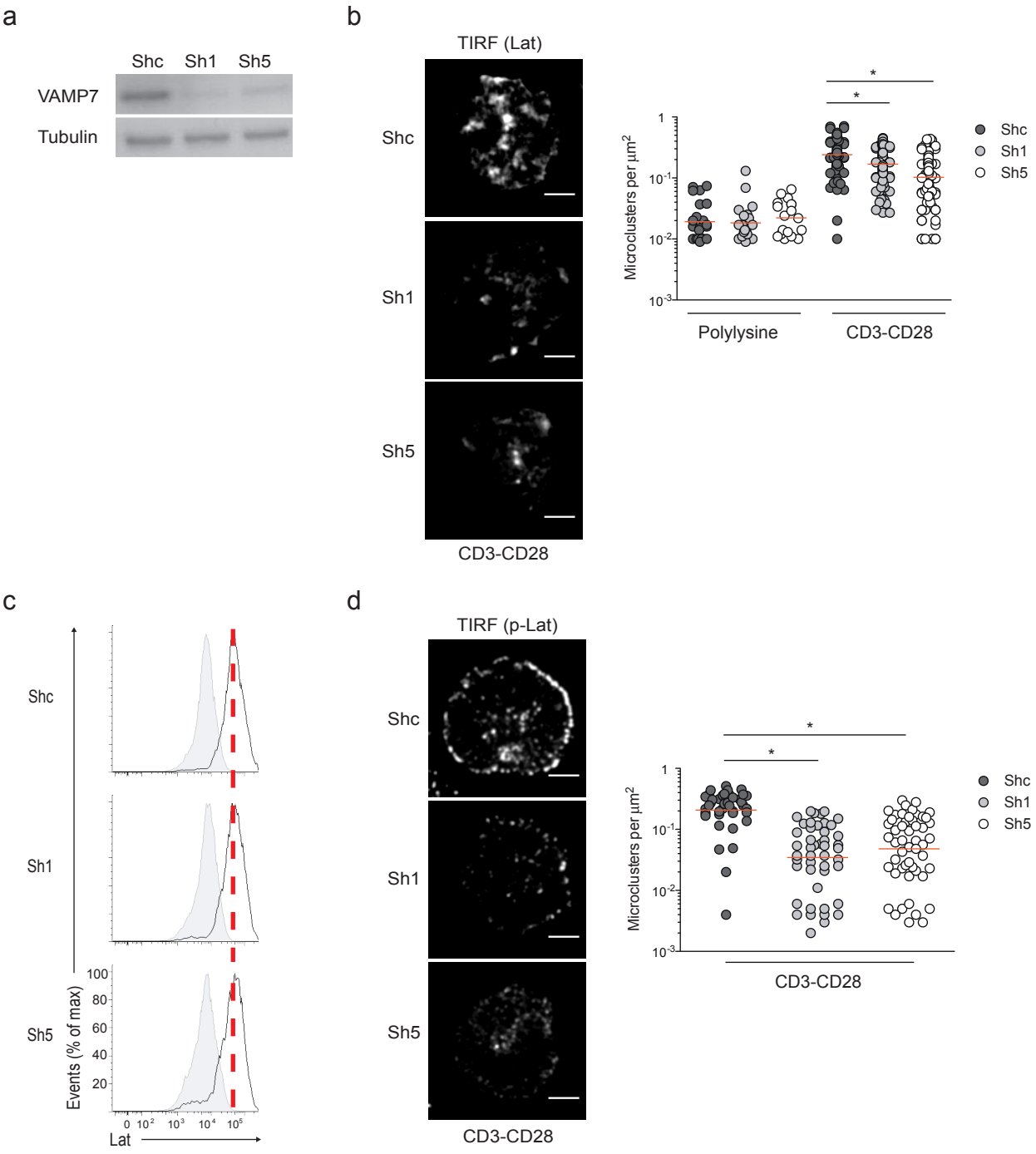

Supplementary Fig.1. **The SNARE molecule VAMP7 controls Lat recruitment to the TCR activation sites in primary human CD4⁺ T cells.** (a) Representative immunoblot analysis of VAMP7 expression in primary human CD4⁺ T cells expressing control (Shc) or VAMP7-specific (Sh1, Sh5) shRNA. (b) Representative TIRF images of endogenous Lat recruitment to the interface between human CD4⁺ cells and anti-CD3 and anti-CD28 mAbs coated coverslips after 10 minutes (left) and quantification of Lat microclusters density (plots). (Shc n=96, Sh1 n=137, Sh5=98). (c) Representative cytofluorimetric analysis of Lat expression in Shc, Sh1 and Sh5 primary human CD4⁺ T cells. (d) Representative TIRF images of phospho-Lat (p-Lat) recruitment to the interface between human CD4⁺ T cells and anti-CD3 and anti-CD28 mAbs coated coverslips after 10 minutes (left) and quantification of p-Lat microclusters density (plots). (Shc n=42, Sh1 n=46, Sh5=51). Red bars: geo mean. Scale bars, 5µm. Student's t-test *p≤0.0001. Data represent 3 experiments (a) or 2 experiments (b-d).

Fig.S1

Nature Immunology doi:10.1038/ni.2609

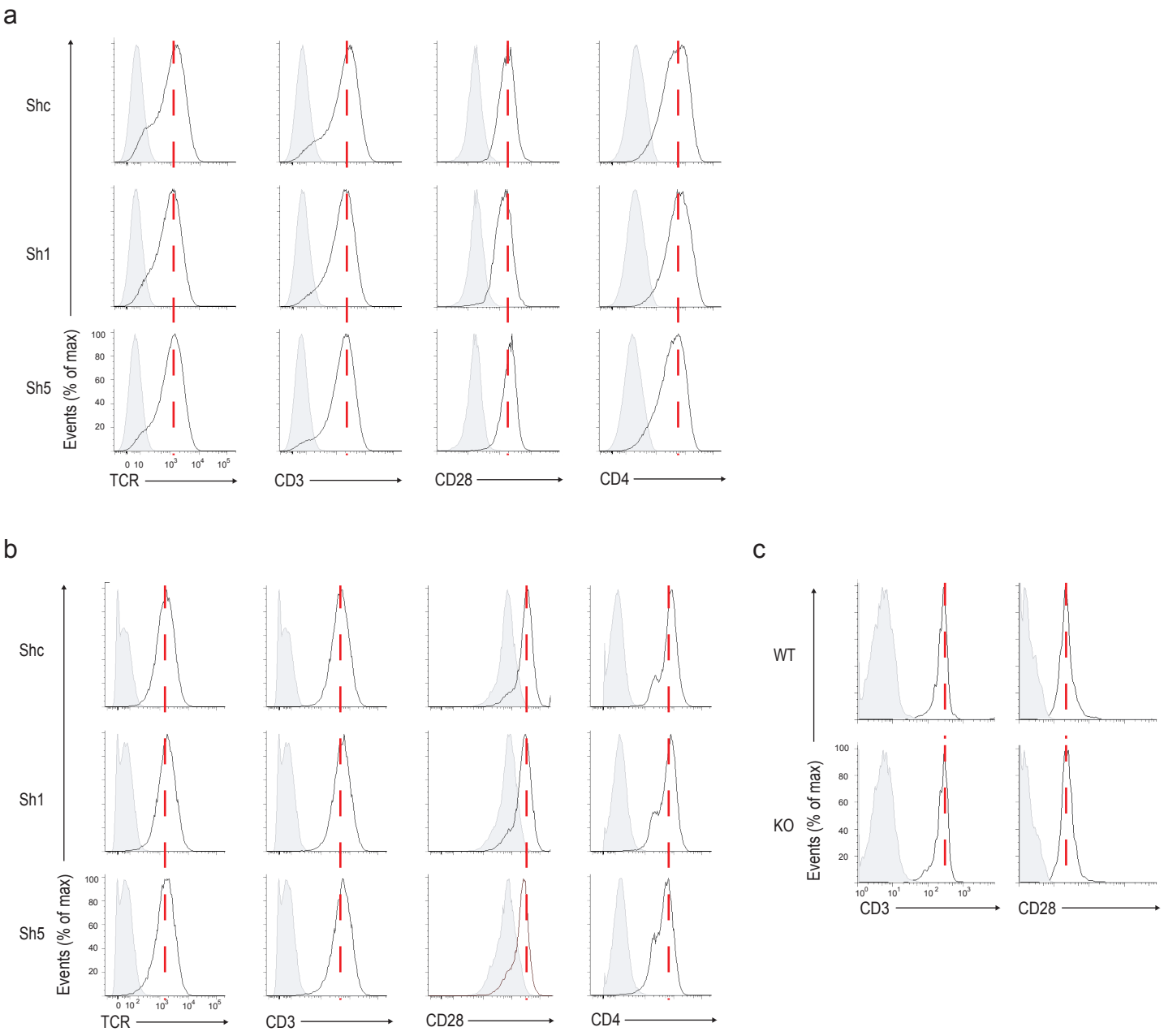

Supplementary Fig.2. **Control of surface markers in VAMP7 silenced Jurkat cells, primary human CD4$^+$ T cells and VAMP7-deficient mouse CD4$^+$ T cells.** (a-c) Cytofluorimetric analysis showing the expression of indicated membrane markers in (a) Jurkat cells or (b) primary human CD4$^+$ T cells expressing control (Shc) or VAMP7-specific shRNAs (Sh1, Sh5) or (c) littermate control (WT) or VAMP7-deficient (KO) mouse purified CD4$^+$ T cells. One experiment representative of 3 is shown (a-c).

Nature Immunology doi:10.1038/ni.2609

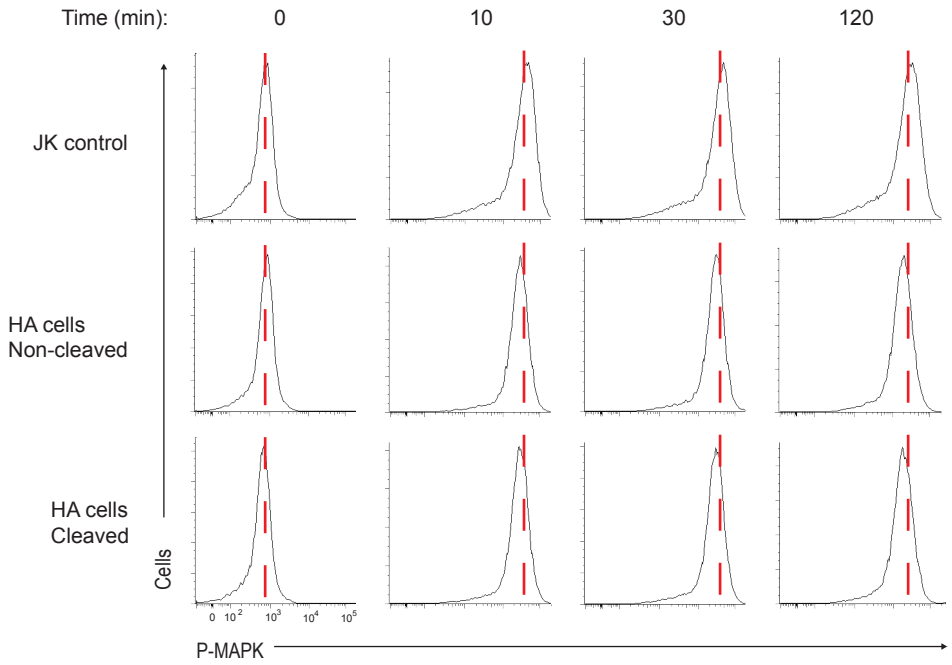

Supplementary Fig. 3. **Jurkat cells expressing HA-TEV-Lat are activated by anti-CD3 and anti-CD28 mAbs.** Cytofluorimetric analysis showing the phosphorylation of MAPK in Jurkat cells (upper row) or Jurkat cells expressing HA-TEV-LAT left untreated (non-cleaved, middle row) or treated with TEV protease (cleaved, lower row). Cells were activated with anti-CD3 and anti-CD28 mAbs for the indicated time, permeabilized and labelled with anti-phospho-MAPK (p-MAPK) Abs. One experiment representative of 3 is shown.

Nature Immunology doi:10.1038/ni.2609

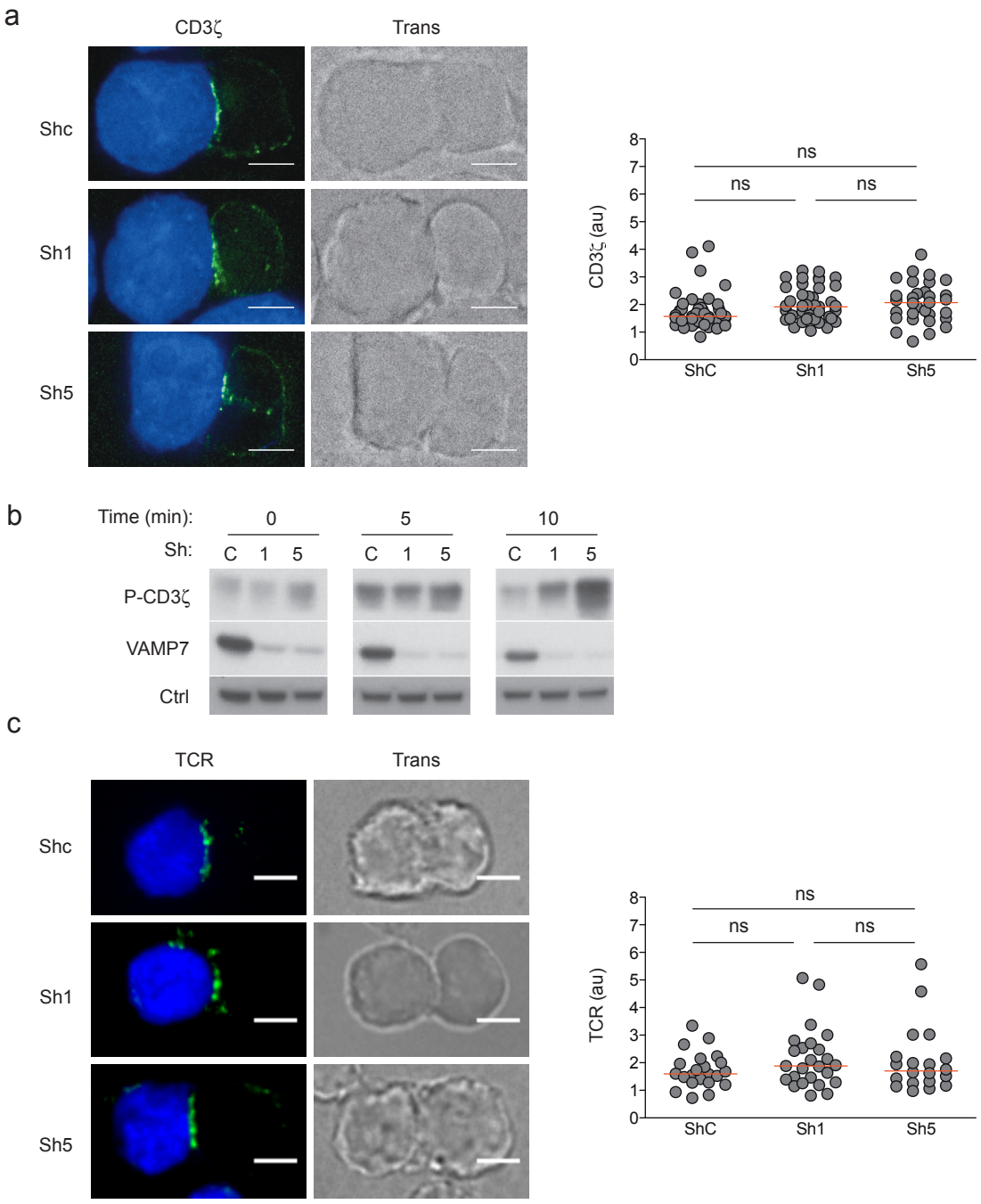

Supplementary Fig. 4. **Vamp7 depletion neither affects CD3ζ nor TCR recruitment to the IS nor CD3ζ phosphorylation.** (a) Representative deconvoluted images of 30 minutes conjugates of Jurkat cells expressing CD3ζ-GFP and SEE-pulsed Raji B cells (in blue)(left). The mean intensity of fluorescence (MFI) of CD3ζ-GFP, on 2 z planes, in a fixed region of the IS was divided by the MFI in the T cell measured on the 2 same z planes. Ratios are expressed in arbitrary unit (au, right), (Shc n=42, Sh1 n=43, Sh5 n=31). (b) Immunoblot analysis of CD3z phosphorylation in Jurkat cells activated with anti-CD3 and anti-CD28 mAbs for the times indicated. (c) Representative deconvoluted images of 30 minutes conjugates of Jurkat cells and SEE-pulsed Raji B cells (in blue)(left). Jurkat cells were labelled at 4°C with anti-TCR antibody prior to fixation, fixed and stained with secondary antibody without permeabilization. Plots show the TCR enrichment at the IS in arbitrary units (au). (Shc n=22, Sh1 n=25, Sh5 n=20). Red bars, median value. Scale bars, 5µm. Student's t-test, ns: non significant. Data are representative of 3 independent experiments (a-c).

Nature Immunology doi:10.1038/ni.2609

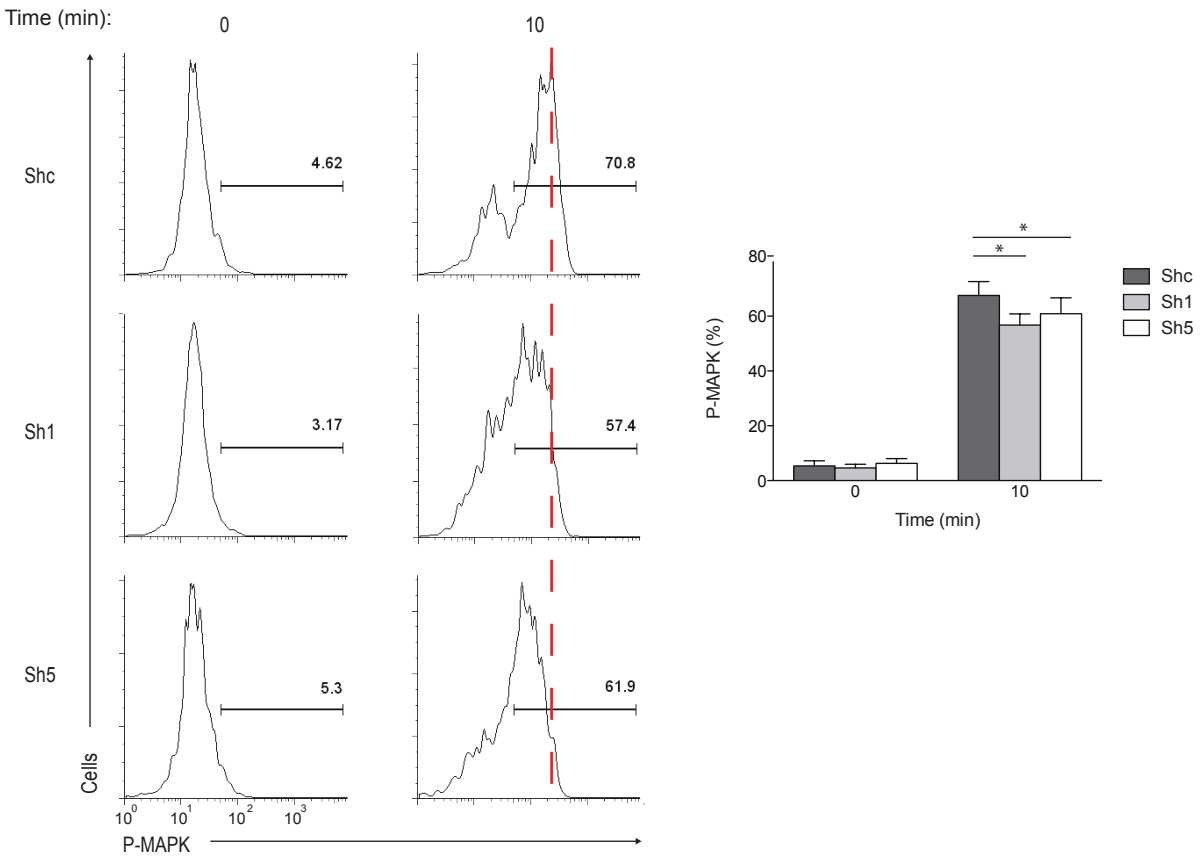

Supplementary Fig.5. **VAMP7 depletion affects MAPK phosphorylation.** Representative cytofluorimetric analysis showing the phosphorylation of MAPK in Jurkat cells expressing control (Shc) or VAMP7-specific shRNAs (Sh1, Sh5), activated with anti-CD3 and anti-CD28 mAbs for 10 minutes, percentage of p-MAPK positive cells are indicated (left). Bars graphs represent mean ± SEM of the percentages of p-MAPK positive cells of 5 independent experiments. Student t test *p≤0.05 (right).

Fig.S5